JOURNAL OF MATERIALS SCIENCE 32 (1997) 5533–5543

In situ hydroxyapatite crystallization for the formation of hydroxyapatite/polymer composites

KOICHI KATO, YOSHIHIRO EIKA, YOSHITO IKADA
Research Center for Biomedical Engineering, Kyoto University, 53 Kawahara-cho, Shogoin, Sakyo-ku, Kyoto 606, Japan

In an attempt to synthesize hydroxyapatite (HAP)/polymer composites, HAP crystallization was investigated in solution in the presence of ionic synthetic polymers. The side groups of the polymers used include carboxylate, dihydrogen phosphate, sulfate, and primary amine. Spontaneous HAP precipitation and amorphous–crystalline transformation occurring in both the presence or absence of ionic polymers were studied by measuring the solution turbidity change and titrating the released protons, respectively. The rates of HAP nucleation and growth were determined from an induction period before onset of crystallization and the subsequent propagation of HAP crystallites. The added anionic and cationic polymers, were found to suppress the crystallization in a concentration-dependent manner. An exception was a concentrated poly(acrylic acid), which was precipitated by calcium ion binding to accelerate the nucleation and the growth of HAP crystallites. These results suggest that a molecular interaction is operative between the ionic polymer chains and the growing HAP crystallites. Infrared spectroscopy and X-ray diffraction analysis revealed that the HAP precipitated in the presence of ionic polymers incorporated the polymer chains in the HAP microcrystalline aggregates. Based on these findings, HAP/poly(acrylic acid) composites were prepared through *in situ* HAP crystallization in the presence of poly(acrylic acid). Tensile testing of the composites and electron microscopic observation of their fractured surfaces revealed that the composite prepared through this wet process was superior to that obtained by simple physical mixing with respect to the wet state mechanical properties and homogeneity in mixing.

1. Introduction

The molecular control of inorganic crystallization by organic substances is a key technology for the fabrication of novel inorganic/organic composites that has recently received a considerable amount of attention [1, 2]. This process mimics biological mineralization in which a preorganized organic phase provides a niche for inorganic crystals to nucleate and grow. Such composite materials prepared through the biomimetic process will offer a wide variety of applications, for instance, in microelectronics, optoelectronics, and biomedical engineering [3]. A number of studies have focused on the effect of functional compounds on the crystallization of hydroxyapatite (HAP) which is the main inorganic component of vertebrate skeletal tissue. Some of these studies have attempted to accumulate fundamental knowledge relevant to the biological calcification mechanism [4–24], since the bone formation seems to proceed through HAP crystallization under molecular regulation by a preorganized organic matrix with respect to its kinetic and spatial aspects. Others have aimed at establishing new approaches for fabricating composite materials to be used for orthopaedic and oral surgery [25–32]. In this case, the HAP component may provide a biocompatible surface which has an ability to firmly bind to bone tissues.

The starting materials employed in these studies on composite formation include low-molecular-weight inorganic [4, 5, 25] and organic [6–11] metabolites and high-molecular-weight natural [12–33] and synthetic [6, 15, 24, 26–32] macromolecules. Most of the macromolecules investigated have a bias toward bone and teeth formation and include collagen [12, 13, 15], bone phosphoprotein [14, 17, 20], dentin phosphoprotein [17], osteonectin [19], bone Gla protein [16], proteoglycan [15], synthetic polypeptides [15, 21, 22, 24], and saliva [18]. However less attention has been paid to the use of synthetic polymers as a component of the composites [34], although they may also have specific effects on the HAP crystallization.

The formation and growth of nuclei for the HAP crystallization are reported to be affected (either inhibited or accelerated) by the organic additives [24, 33]. The main roles that the added organic polymers play in the composite formation are thought to be

0022–2461

structural control on the morphology, size, and anisotropy of generated inorganic crystals and their distribution over the organic phase [24, 33]. Kinetic data taken for the HAP crystallization can provide evidence for molecular interactions between the inorganic crystals and the added organic molecules. Structural studies on inorganic/organic composites can be helpful in elucidating the micro- and macroscopic structure of calcified tissues and consequently an understanding of their superior mechanical properties. Such studies can also provide practical information for fabricating inorganic/organic composites through biomimetic processes.

The major aim of the present study is to gain a deep insight into the HAP crystallite formation from supersaturated calcium phosphate solutions in the presence of synthetic ionic polymers in order to fabricate HAP/polymer composites. In particular, poly(acrylic acid) (PAAc) is employed as the organic additive, because of its ability to strongly bind calcium ions. The HAP crystallization will be kinetically studied in the presence of PAAc. For comparison with the HAP/PAAc composite fabricated using a three-dimensional PAAc gel, a simple physical mixing method is employed to fabricate a HAP/PAAc composite. Finally, the microstructure and tensile properties of the resultant composites will be briefly studied.

2. Experimental procedures

2.1. Chemicals

Calcium chloride dihydrate and anhydrous disodium hydrogenphosphate both of an extra pure grade were purchased from Wako Pure Chemical Industries Co. Ltd., Japan, and used as received. Acrylic acid (AAc) and methacryloyl-poly(oxyethylene) phosphate (MPOP) monomers were obtained from Wako Pure Chemical Industries Co. Ltd. and Unichemical Co. Ltd., Japan, respectively. The AAc monomer was purified by the conventional distillation method prior to use. The poly(acrylic acid) (PAAc) that had average molecular weights ($\bar{M}_w$) of 4.5×10^5, 1.0×10^6, and 4.0×10^6 were obtained from Polyscience, USA, whilst an additional PAAc with an $\bar{M}_w$ of 1.0×10^4 was prepared in our laboratory by conventional free radical polymerization techniques. The poly(2-acrylamido-2-methyl propane sulfonic acid) (PAMPS) and polyallylamine (PAA) were obtained from Nitto Chemical Industry Co. Ltd., Japan. The chemical structure of the polymers used in this study is presented in Fig. 1.

2.2. Preparation of the AAc-MPOP copolymer

The free radical copolymerization of MPOP and AAc was carried out at three different feed concentration ratios of 0:5.0, 0.5:4.5, and 3.0:2.0 (MPOP/AAc, w/w). A Pyrex glass ampoule containing an aqueous monomer solution with a total monomer concentration of 5.0 wt %, 0.05 wt % potassium persulfate (initiator), and 0.01 wt % L-cysteine (chain transfer agent) was sealed after degassing. The sealed ampoule

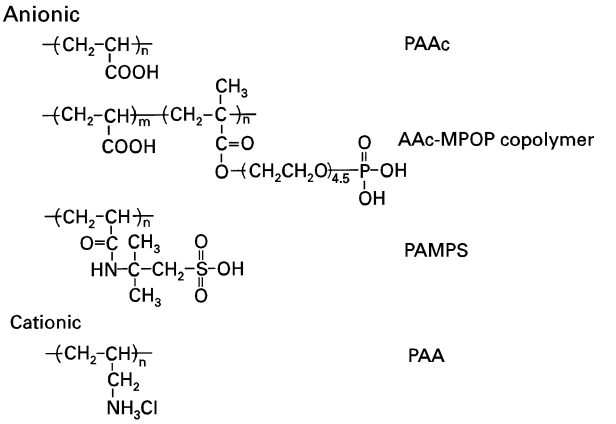

Figure 1 Chemical structure of the ionic polymers used in this study.

was kept at 50 °C for 40 min in order to effect free radical copolymerization and the resulting water-soluble copolymers were recovered by precipitation with a large amount of acetone. The mole fraction of MPOP units in the copolymers was determined, using the molybdenum blue method [35], to be 0.00 (PAAc), 1.67, and 5.41 MPOP mol %.

2.3. Kinetic study of the HAP crystallization

A kinetic study of the HAP precipitation was performed in the presence of polymers by mixing two solutions of calcium chloride and disodium hydrogen phosphate at two different concentrations (systems I and II) under a fixed Ca/P molar ratio of 5:3. For all the precipitation studies the water used for the medium preparation was deionized, double-distilled, and filtered through a Milipore MG-X membrane.

2.3.1. System I

The solution used in system I is characterized by its significantly lower concentration product of calcium and phosphate ions than the solution used in system II as is further described below. The aqueous solution of 2.45 mM disodium hydrogen phosphate and that of 200 mM calcium chloride were prepared separately, stored at 4 °C, and used within 1 week after preparation. These solutions were buffered with a 0.1 mM 2-amino-2-hydroxymethyl-1,3-propanediol and hydrogen chloride (tris-HCl buffer) (pH 7.4). Each of the polymers was dissolved in 19.6 ml of the disodium hydrogen phosphate stock solution under stirring and then kept at 30 °C. To this polymer solution, 0.4 ml of the calcium chloride stock solution was added and the time of addition was recorded as time zero. The mixed solution was stirred with a teflon-coated magnetic stirrer under a constant rotation of 400 r.p.m. at 30 °C. The initial calcium and phosphate concentrations were 4.0 and 2.4 mM, respectively. The solution appeared clear shortly after mixing, but became turbid after a period of time and yielded a precipitated solid phase. The solution turbidity was recorded with a spectrophotometer (Shimadzu UV-1200, Kyoto, Japan) at 500 nm and plotted against time after mixing.

2.3.2. System II

The aqueous solutions of 7.2 mM disodium hydrogen phosphate and 60 mM calcium chloride were prepared separately, stored at 4 °C, and used within 1 week after preparation. Each of the polymers was dissolved in 250 ml of the disodium hydrogen phosphate stock solution in a 3-necked round flask equipped with a thermometer, a pH electrode (6366-10D, Horiba, Kyoto, Japan) connected with a pH meter (pH meter F-14, Horiba, Japan), and a microburette and then the resulting solution was kept at 20 or 25 °C. The pH electrode was freshly equilibrated using pH standard buffer solutions. To this polymer solution, 50 ml of the calcium chloride stock solution was added and similar to system I, this time was recorded as time zero. The initial calcium and phosphate concentrations were 10 and 6 mM, respectively. The mixed solution became turbid upon mixing due to the formation of precipitates of amorphous calcium phosphate. The pH of the mixed solution was adjusted to 7.40 by adding 5.0 N NaOH solution within 30 s of the mixing. The solution pH started to drop after a period of time, because an amorphous–crystalline transformation occurred with a release of protons. The pH was maintained at 7.40 $\pm$0.05 by adding 0.1 N NaOH and the amount of the titrant added was measured using a microburette after mixing.

2.4. Characterization of the precipitates

The precipitates formed in systems I and II were immediately separated from the aqueous medium by centrifugation to avoid any additional transformation. After freeze-drying, the Fourier-transform infrared (FT-IR) absorption spectrum of precipitates was recorded on an FT-IR 8000 Spectrometer (Shimadzu Corp., Kyoto, Japan) at a resolution of 4 cm^{-1} using the KBr pellet technique. The morphology of the precipitates was observed after coating of the samples with a thin layer of platinum with a scanning electron microscope (SEM) (S-450, Hitachi, Japan) operated at 15 kV. A powder X-ray diffraction (XRD) pattern of the precipitates was recorded with a RAD-X diffractometer (Rigaku International Corp., Tokyo, Japan) (X-ray: Cu$K_{\alpha 1}$) operated at 40 kV, 30 mA, and a scan speed of 2.0° min^{-1}. Sintered HAP powders were used as a standard.

To investigate the adsorption of the ionic polymers onto the HAP surface, a suspension of the HAP powders formed in system II was mixed with an ionic polymer solution. The concentrations of the HAP and ionic polymer were kept at 1.0 and 0.2 wt %, respectively. The adsorption of the suspension at 500 nm 1 min after addition of the polymer solution was recorded as the turbidity.

2.5. Composite preparation

HAP/PAAc composites were prepared through two different methods; physical mixing and *in situ* mixing.

Physical mixing between the HAP powders formed in system II in the absence of polymers and PAAc powders was performed in a mortar with a pestle in the dry state. The HAP/PAAc ratio was fixed at 40:60 by weight. The mixed powders were then compression-moulded under 20 MPa at 25 °C.

For the HAP/PAAc composite preparation through *in situ* mixing, the precipitates formed in system II in the presence of 10 mM PAAc were used as a starting material. They were compressed in the same manner as described above. The HAP content in the precipitates was 40 wt %. Tensile testing of the above two HAP/PAAc composites was performed in both dry and wet states with an Autograph type AGS-D tester (Shimadzu Corp.) at a constant crosshead speed of 1 mm min^{-1} and 25 °C under a 60% relative humidity (RH). The wet specimens tested were obtained by soaking the dry composites in water for 0–10 min at 25 °C.

Another composite was prepared through *in situ* HAP crystallization in the presence of a PAAc hydrogel prepared by copolymerizing an AAc monomer with *N*,*N*-methylene-bis-acrylamide using 0.2 wt % ammonium persulfate and 0.1 wt % *N*,*N*,*N*′,*N*′-tetramethylethylenediamine. The content of the crosslinker was 10 wt % of AAc. To a 200 mM calcium chloride solution (pH 7.4) containing the PAAc gel, 120 mM of disodium hydrogen phosphate solution (pH 7.4) of equal volume was added and the mixture was kept at 25 °C for 48 h under mild shaking in order to deposit HAP inside the gel. The back-scattered image and X-ray image of the calcium atoms were taken on carbon coated fractured surfaces of the composite with an electron microprobe analyser (EMA) (Shimadzu Corp.) operated at an accelerating voltage of 20 kV.

3. Results

The physicochemical properties of inorganic/organic composites are largely governed by the interfacial structure between the inorganic and organic phases, which is a function of the compatibility between the two different phases. In order to quantitatively study this compatibility, aqueous solutions of various polymers were added to aqueous suspensions of the HAP powders. It is expected that the turbidity of an HAP suspension changes on polymer addition if there is any interaction between the HAP surface and the added polymer. Fig. 2 shows an SEM photograph of the HAP powders used for the physical mixing and Table I lists the turbidity changes observed when 10 ml of 0.2 wt % polymer solution in 0.1 M tris-HCl buffer of pH 7.4 was added to 10 ml of 1 wt % HAP suspension. Since the turbidity changed very rapidly on solution addition, the absorption was measured 1 min after addition. The absorption of the HAP suspension before the addition of the polymer solutions was 1.301. As can be seen from Table I, the suspension turbidity decreased when the PAAc or AAc-MPOP copolymer solutions were added, but increased on the addition of the PAMPS and PAA solutions. Evidently, the reduction in the turbidity is due to the coagulation of HAP particles caused by polymer adsorption onto their surface, followed by precipitation to the

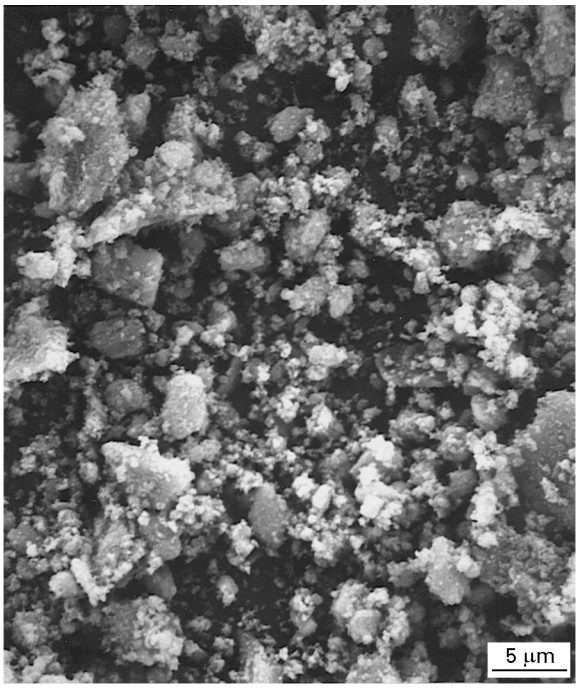

Figure 2 Scanning electron micrograph of the HAP powders formed under the condition of system II in the absence of polymers (these powders were used for the physical mixing with PAAc).

TABLE I Coagulation of HAP particulates upon addition of ionic polymers to the HAP suspension

Polymer	Ionic group in the polymer	Anionic or cationic	Solution turbidity
None	—		1.301
PAAc	Carboxylic acid	Anionic	0.130
AAc–MPOP copolymer	Carboxylic acid-Dihydrogen phosphate	Anionic	0.295
PAMPS	Sulfonic acid	Anionic	1.859
PAA	Primary amine	Cationic	1.805

vessel bottom, resulting in the creation of a less turbid supernatant. On the other hand, the turbidity increase may be ascribed to the incorporation of the added polymer molecules to the suspension without precipitation.

3.1. Physical mixing

Since PAAc showed the largest turbidity change with the polymer addition, composite preparation using physical mixing was attempted using PAAc. Fig. 3 shows the back-scattered electron micrograph of the fractured surface of the composite made from PAAc and HAP powders by pressing a mixture of these powders at room temperature. The composite was very brittle, as expected from the rough surface noticed in Fig. 3. When a composite was prepared by casting a PAAc solution containing suspended HAP powders, followed by drying, the resulting composite film was much more brittle than that prepared by pressing. This is probably because mixing of the HAP powders with the PAAc phase was extremely inhomogeneous due to HAP aggregation by PAAc, as is suggested by the results listed in Table I.

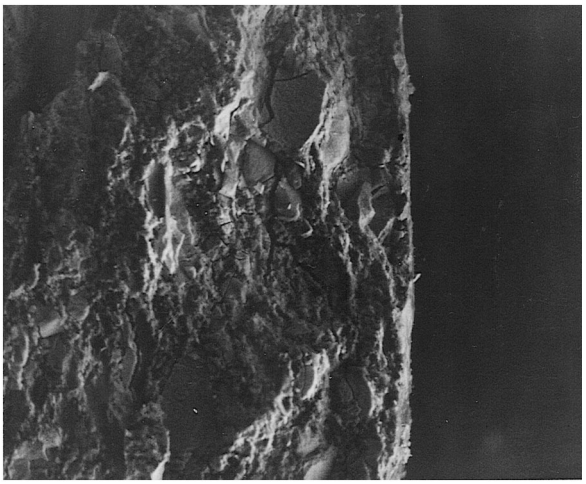

Figure 3 Back-scattered electron micrograph of the fractured surface of the HAP/PAAc composite prepared through physical mixing.

3.2. *In situ* mixing

In order to improve the mixing of the two phases, we attempted to create HAP particulates from Ca^{2+} and PO_4^{3-} ions in the presence of soluble PAAc. In other words, solid HAP was deposited from a saturated salt solution containing PAAc.

3.2.1. Deposition kinetics

The deposition of HAP from an aqueous PAAc solution containing the saturated salt was performed at two different solute concentrations: low (system I) and high (system II).

In system I, the plot of solution turbidity against the stirring time after mixing of disodium hydrogen phosphate solution with calcium chloride solution gave a sigmoidal curve, regardless of the presence or absence of PAAc. Fig. 4a shows the curves, which may be divided into two distinct regions; the clear solution region before onset of the spontaneous precipitation and the turbid solution region associated with calcium phosphate precipitation. The induction time (T_{pre}) before onset of the precipitation was determined from the point where the extrapolated linear curve of the increased turbidity part (b in Fig. 5) intersected the extrapolated linear curve of the constant turbidity part (a in Fig. 5). The inverse of the induction time was defined as the nucleation rate in this study. The apparent rate (R_{pre}) of precipitate formation or growth in the initial stage was determined from the slope of the linear curve (b) in Fig. 5. Also in system II, the plot of NaOH uptake after mixing of the two solutions exhibited similar two regions, as presented in Fig. 4b, although instantaneous precipitation was observed on the addition of the phosphate solution to the calcium chloride solution. Until a rapid increase in the NaOH consumption, the solution pH remained constant. The induction time (T_{trans}) before onset of

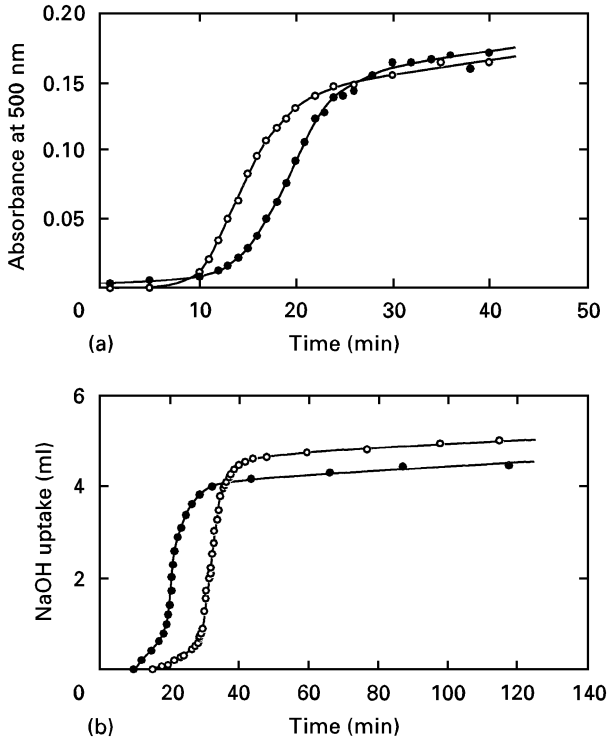

Figure 4 Time course of the HAP crystallization in; (a) system I ([Ca] = 4 mM, [PO_4] = 2.4 mM, [polymer] = 0.02 mM, 30 °C) and (b) system II ([Ca] = 10 mM, [PO_4] = 6 mM, [polymer] = 5 mM, 20 °C) in the presence of PAAc (●) and in the absence of polymers (○).

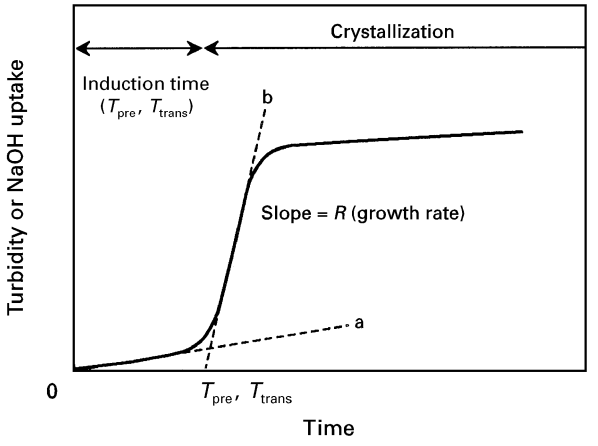

Figure 5 Schema for determining the induction time (T_{pre}, T_{trans}) and the growth rate (R_{pre}, R_{trans}) of HAP crystallization from a time–conversion curve.

the transformation was determined from the point where the extrapolated linear curve of the NaOH uptake part (b in Fig. 5) intersected the extrapolated curve of the constant NaOH uptake part (a in Fig. 5). The apparent rate (R_{trans}) of the initial transformation (growth) was determined from the slope of the linear curve (b) in Fig. 5, similar to R_{pre} in system I.

Table II summarizes the kinetic data on the crystallization of HAP in the presence and absence of PAAc, together with those of other polymers. The MPOP homopolymer is not included in Table II due to its very poor solubility in aqueous media. It can be seen from Table II that the addition of polymers to system I mostly prolonged the induction period whilst the growth rate exhibited no significant change. The result suggests that these ionic polymers inhibit the HAP nucleation. In system II, the amorphous–crystalline transformation was significantly enhanced by the addition of PAAc, whereas the addition of the other polymers gave the opposite result. It should be noted that the 5 mM PAAc added in system II underwent aggregation on mixing with the calcium chloride solution, whereas the other polymers did not form such aggregates. The addition effect of the cationic PAA was not significant in system I, but a strong inhibition of the transformation into HAP was observed in system II.

The dependence of the nucleation and growth rate of HAP on the monomer unit concentration of PAAc with $\bar{M}_w$ of 4.5×10^5 is plotted in Fig. 6 (a and b). In system I, an increase in the PAAc concentration clearly led to a significant decrease in the nucleation rate and a slight reduction in the growth rate. A further increase in the PAAc concentration from 0.06 mM resulted in no induction of HAP crystallization in system I. On the contrary, the nucleation and growth rate of HAP slightly increased with an increasing concentration of PAAc in system II.

Fig. 7 (a and b) shows the effect of the molecular weight of the PAAc. Apparently, in system I, the influence of the PAAc molecular weight on the growth rate is unremarkable, although the nucleation rate became significantly higher when PAAc with a $\bar{M}_w$ of 4.5×10^5 was added. In system II, the nucleation rate was not influenced to a large extent by the molecular weight, while the growth rate considerably increased with an increase in the PAAc molecular weight. The addition of the AAc monomer (molecular

TABLE II Addition effects of ionic polymers on the induction period (T_{pre}, T_{trans}) and the growth rate (R_{pre}, R_{trans}) of HAP crystallization

Polymer	System I [a]		System II [a]	
	T_{pre} (min)	R_{pre} (min^{-1})	T_{trans} (min)	R_{trans} (ml min^{-1})
None	9.8	14.9	28.6	0.574
PAAc [b]	14.3	14.6	19.3	0.802
AAc–MPOP [c] copolymer	32.5	12.3	24.9	0.263
PAMPS	16.4	22.5	40.7	0.466
PAA	9.0	12.7	29.9	0.065

[a] Precipitation condition: system I: [Ca] = 4 mM, [PO_4] = 2.4 mM, [polymer] = 0.02 mM, 30 °C. System II: [Ca] = 10 mM, [PO_4] = 6 mM, [polymer] = 5 mM, 20 °C.
[b] $\bar{M}_w$ = 450 000.
[c] MPOP content = 5.41 mol %.

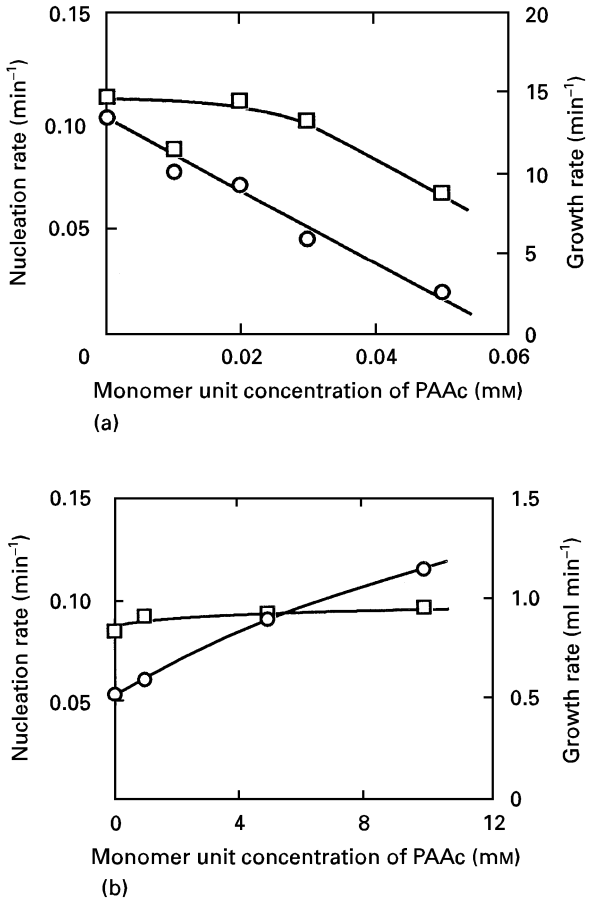

Figure 6 Effects of the PAAc concentration on the nucleation rate (○) and the growth rate (□) of HAP crystallization in; (a) system I ([Ca] = 4 mM, [PO_4] = 2.4 mM, 30 °C) and (b) system II ([Ca] = 10 mM, [PO_4] = 6 mM, 25 °C). The $\bar{M}_w$ of the added PAAc was 450 000.

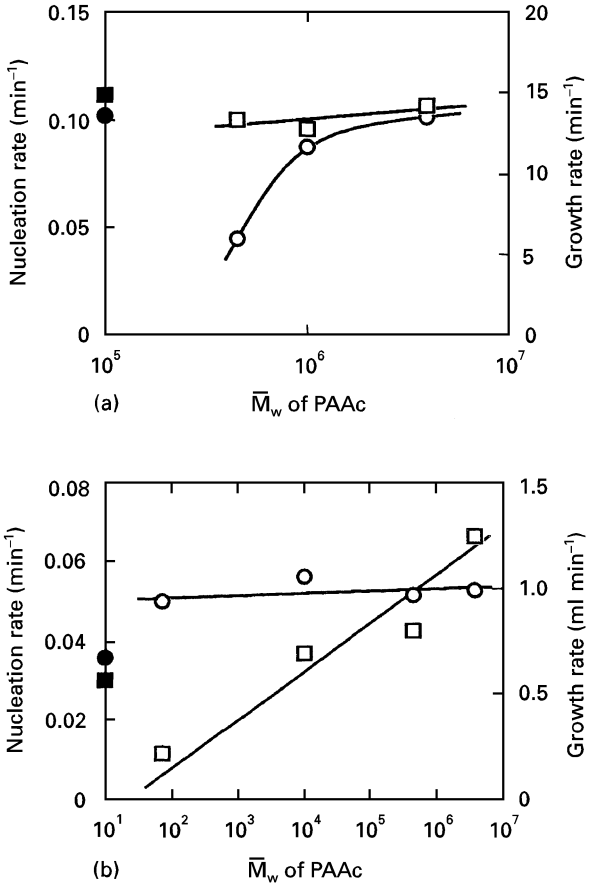

Figure 7 Effects of the average molecular weight ($\bar{M}_w$) of PAAc on the nucleation rate (○) and the growth rate (□) of HAP crystallization in; (a) system I ([Ca] = 4 mM, [PO_4] = 2.4 mM, [polymer] = 0.03 mM, 30 °C) and (b) system II ([Ca] = 10 mM, [PO_4] = 6 mM, [polymer] = 5 mM, 20 °C). Filled symbols (●,■) indicate the results obtained in the absence of polymers. Plots at $\bar{M}_w$ = 72 in system II correspond to the AAc monomer.

weight = 72), which was not precipitated on the addition of calcium ions, effectively reduced the growth rate, while PAAc with a $\bar{M}_w$ higher than 1×10^4, that was precipitated due to binding with calcium ions, enhanced the growth rate of HAP in a $\bar{M}_w$-dependent manner. As is shown in Table II, copolymerization of AAc with a small amount of MPOP greatly reduced the HAP growth rate in system II. To confirm this copolymerization effect, the deposition kinetic parameters were determined for the AAc–MPOP copolymers with different MPOP contents. The result is shown in Fig. 8 (a and b). The $\bar{M}_w$ of the copolymers were almost similar to each other, when assessed from the solution viscosity. The copolymers were water-soluble and underwent no further precipitation by calcium binding, although incorporation of the phosphate monomer into the copolymers was very low. An increase in the mole fraction of dihydrogen phosphate in the copolymers gave rise to a low nucleation rate and a low growth rate in both systems I and II, in comparison with the addition of the AAc homopolymer.

3.2.2. Structure of the precipitates

FT-IR spectra of the precipitates formed in systems I and II are presented in Figs 9 and 10, respectively. As is shown in Fig. 9, the precipitates collected 40 min after solution mixing show typical IR spectra characteristic of poorly crystallized HAP. The crystallization of the precipitated HAP is supported by the split antisymmetric absorption bands observed at around 600 cm^{-1} [36]. No significant changes in the IR spectrum due to the PAAc addition to system I was observed which is probably due to the quite low concentration of PAAc involved in the precipitation. On the other hand, spectra of the HAP precipitated in system II in the presence of PAAc have peaks that are assigned to both HAP (560, 600, 960 and 1040 cm^{-1}), and ionized PAAc (1170, 1250, 1410, 1450 and 1650 cm^{-1}), as is shown in Fig. 10, where the IR spectra of acid-type and partially dissociated PAAc are also presented. The peak at 1560 cm^{-1} can be assigned to the antisymmetric mode of the carboxylate ion, while the peak at 1710 cm^{-1} can be assigned to the carbonyl stretching vibration mode. This peak is shifted to 1560 cm^{-1} upon dissociation. As can be seen in the spectra taken before the transformation, the peak at 1560 cm^{-1} also appears in the precipitates collected just after mixing, suggesting that calcium ions have bound instantaneously to the PAAc before the HAP crystallization starts. XRD patterns of the precipitates formed under different conditions in system II are shown in Fig. 11. As can be seen in patterns a–c the precipitates collected 10 min after mixing of

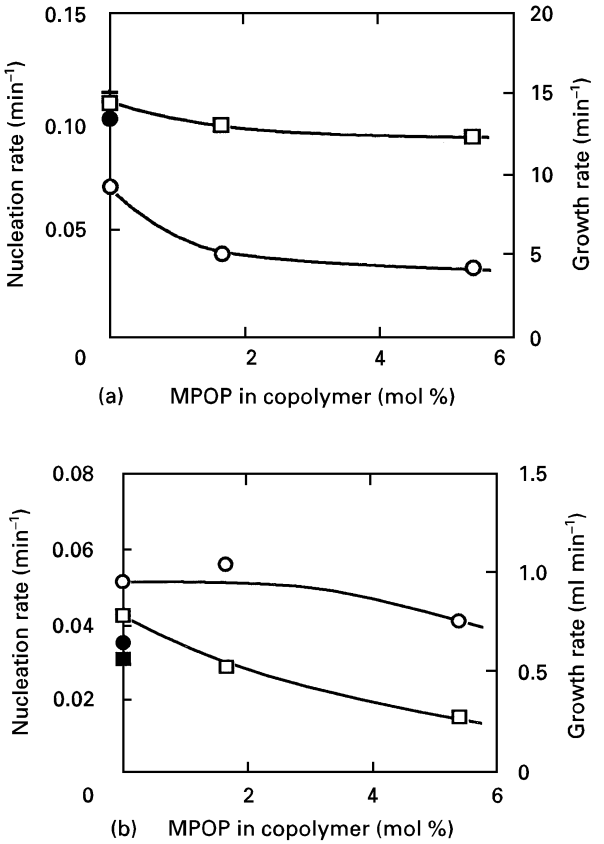

Figure 8 Effects of the dihydrogen phosphate side group on the nucleation rate (○) and the growth rate (□) of HAP crystallization in; (a) system I ([Ca] = 4 mM, [PO_4] = 2.4 mM, [polymer] = 0.02 mM, 30 °C) and (b) system II ([Ca] = 10 mM, [PO_4] = 6 mM, [polymer] = 5 mM, 20 °C). Filled symbols (●,■) indicate the results obtained in the absence of polymers.

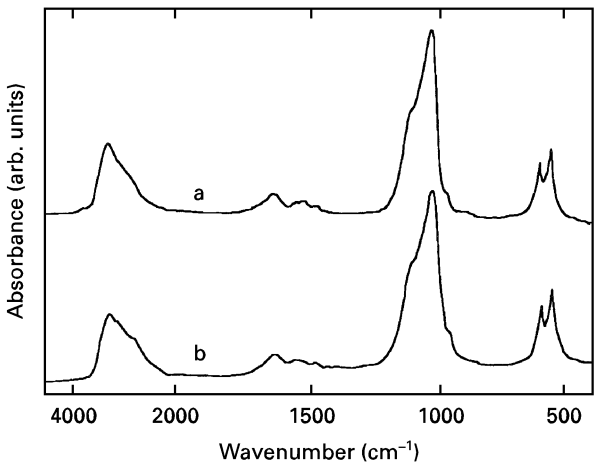

Figure 9 FT-IR spectra of precipitates formed in system I ([Ca] = 4 mM, [PO_4] = 2.4 mM, [polymer] = 0.02 mM, 30 °C, 40 min). (a) in the absence of polymers and (b) in the presence of PAAc ($\bar{M}_w$ = 450 000).

the two solutions in the absence of any polymers have a diffraction pattern that is characteristic of the amorphous form of HAP, whereas those after 2 h reaction show apatitic peaks. Prolongation of the reaction up to 48 h did not cause any further appreciable changes in the diffraction patterns, as is apparent from pattern c, although a gradual NaOH uptake still continued after 2 h. These findings indicate that

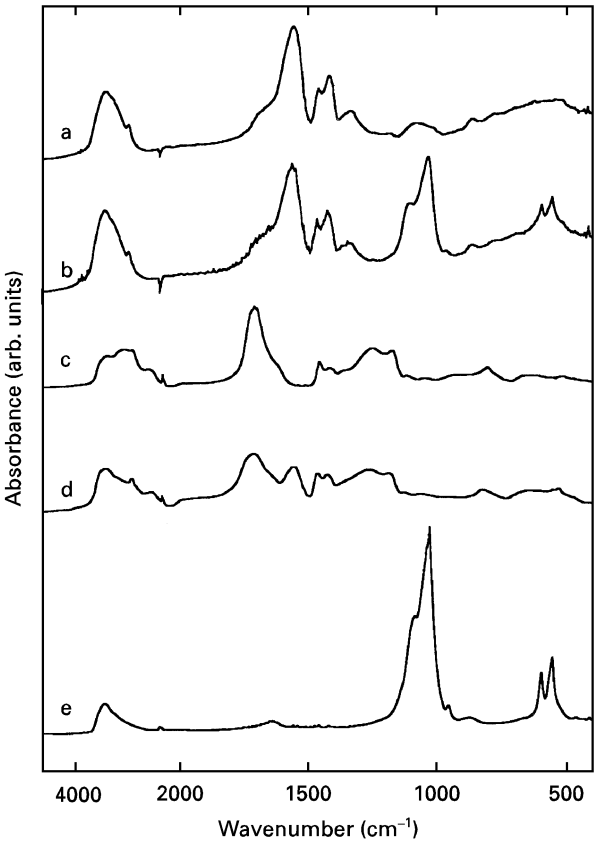

Figure 10 FT-IR spectra of HAP formed in both the presence and absence of PAAc in system II ([Ca] = 10 mM, [PO_4] = 6 mM, 25 °C). (a) and (b) in the presence of 10 mM PAAc ($\bar{M}_w$ = 450 000). The precipitates were collected (a) before and (b) after HAP transformation; (c) undissociated PAAc; (d) partially dissociated PAAc and (e) HAP formed in the absence of polymers.

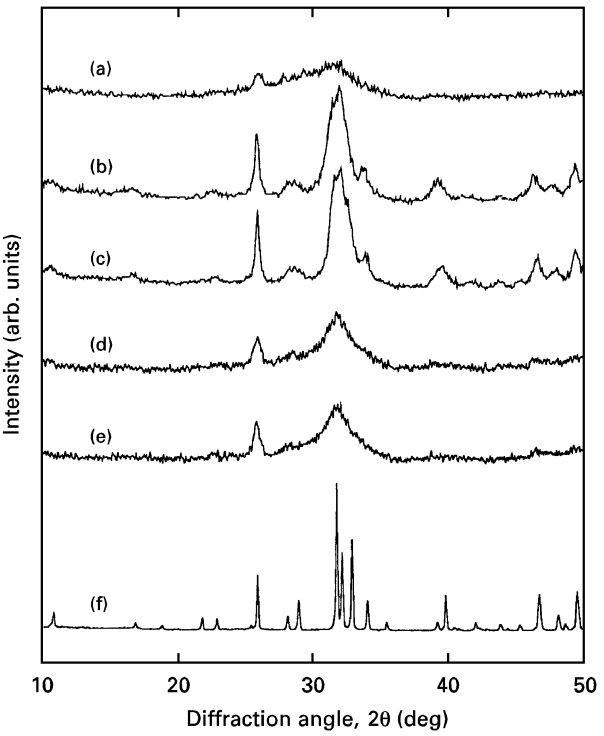

Figure 11 XRD patterns of the precipitates formed in system II ([Ca] = 10 mM, [PO_4] = 6 mM, [polymer] = 5 mM, 25 °C) precipitated (a) 30 s; (b) 2 h and (c) 48 h after addition of calcium chloride to disodium hydrogen phosphate solution in the absence of polymers; (d) precipitated after 2 h in the presence of PAAc ($\bar{M}_w$ = 450 000) and (e) AAc-MPOP copolymer (MPOP content = 5.41 mol %) (f) sintered HAP powders.

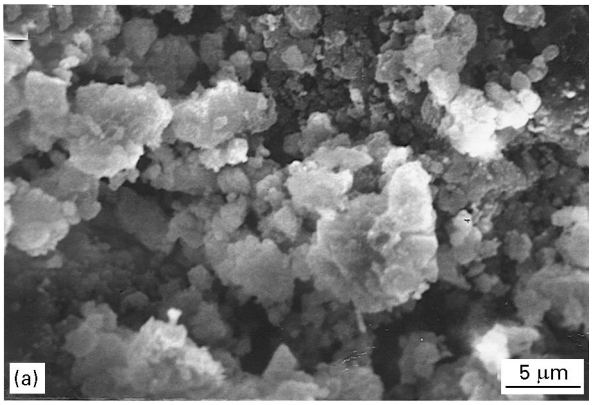

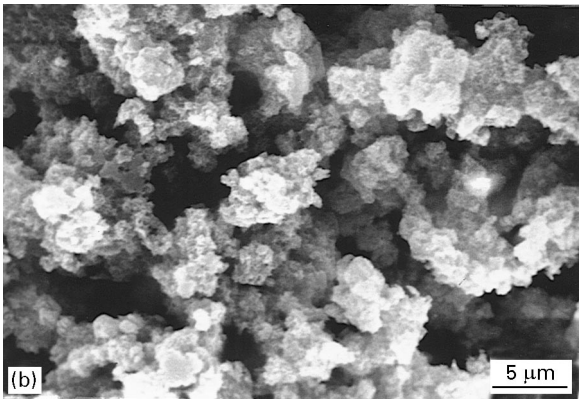

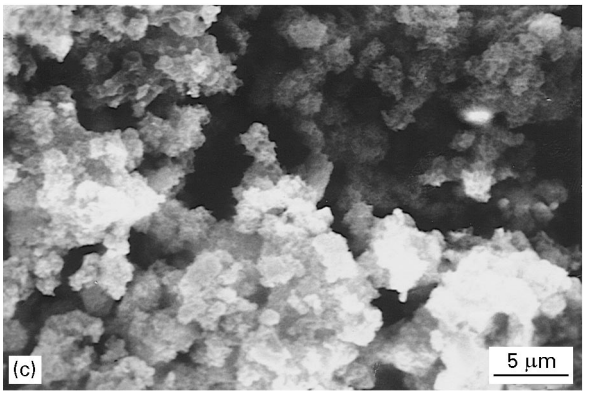

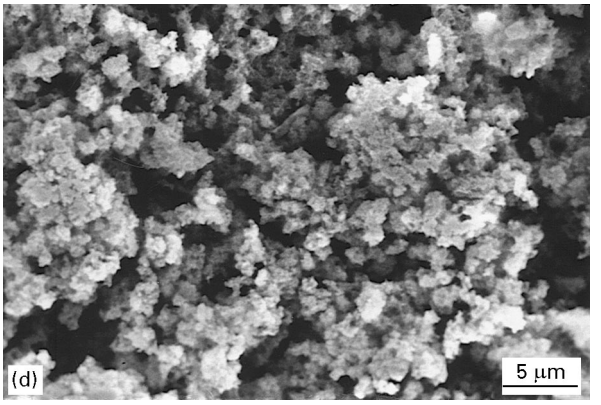

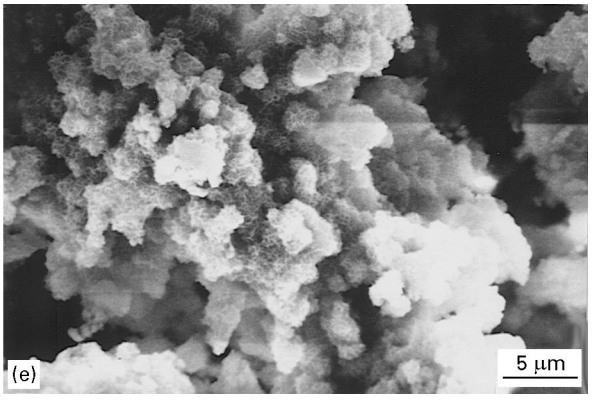

Figure 12 Scanning electron micrographs of the precipitates formed in system I ([Ca] = 4 mM, [PO_4] = 2.4 mM, [polymer] = 0.02 mM, 30 °C, 1 hr). (a) in the absence of polymers (b) in the presence of PAAc ($\bar{M}_w = 450\,000$); (c) AAc-MPOP copolymer (MPOP content = 5.41 mol %); (d) PAMPS and (e) PAA.

the rapid increase in NaOH uptake is observed 15–30 min after mixing of the two solutions is a consequence of the phase transition of amorphous calcium phosphate into HAP. The broad nature of the peaks in the diffraction pattern may be a result of the relatively low reaction temperature [37]. On the other hand, the precipitates formed in the presence of PAAc 2 h after solution mixing showed much more diffuse diffraction patterns than those formed in the absence of polymers. As is shown in the diffraction patterns d and e, when PAAc and the AAc-MPOP copolymer were added, the polymers were incorporated into the HAP aggregates. Fig. 12(a–e) shows scanning electron microphotographs of the HAP deposited in system I both in the absence and presence of ionic monomers. Apparently, the precipitates consist of small aggregates. Other polymers yielded HAP precipitates with a morphology quite similar to that of PAAc, with the exception of PAMPS which produced an assembly of smaller particulates than the others, as shown in Fig. 12d.

3.2.3. Composite from PAAc gel

Based on the HAP deposition kinetics observed for system II, we attempted to prepare HAP/PAAc composites through *in situ* HAP crystallization in the presence of PAAc. The precipitates formed were pressed at room temperature to obtain a composite with a HAP/PAAc weight ratio of 40:60. The tensile strength in the wet state is plotted against the time immersed in water in Fig. 13, together with that of the composite prepared by simple physical mixing to have the same HAP/PAAc ratio. The strength at time zero is equal to that of composites in the dried state. Clearly, the *in situ* deposition method provides a HAP/PAAc composite with a higher resistance to water, although the dry state tensile strength was much lower than that prepared by physical mixing.

A crosslinked PAAc gel was also used for composite preparation using *in situ* crystallization. The PAAc gel was immersed in an aqueous solution containing phosphate and calcium ions at oversaturated concentrations to deposit HAP precipitates inside the water-swollen PAAc gel. The resulting HAP/PAAc gel composite was dried and the fractured surface was observed by back-scattered electron microscopy. Fig. 14(a) shows the result. Comparison of Fig. 14(a) with Fig. 3 clearly reveals that the HAP precipitates are homogeneously dispersed throughout the cross-section of the compact composite in marked contrast with that prepared through physical mixing. An EMA

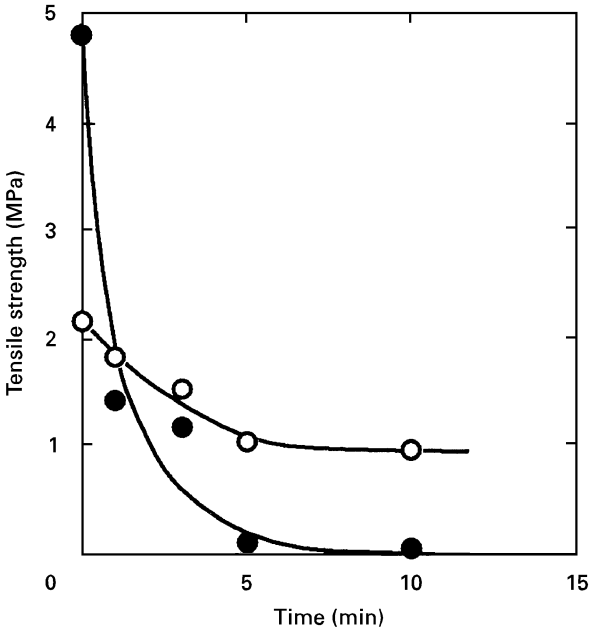

Figure 13 Tensile strength of HAP/PAAc composites prepared through: (○) *in situ* HAP crystallization and (●) physical mixing as a function of the soaking time in water.

result of this composite is shown in Fig. 14(b), where it can be seen that the calcium in the fine HAP particles are homogeneously dispersed in the PAAc matrix.

4. Discussion

Although details of the formation mechanism of biological inorganic/organic composites such as bone tissue are still covered with a thick veil, it seems probable that deposition of the inorganic phase on the organic matrix is controlled by non-collagenous proteins or glycosaminoglycans adsorbed on the surface of the organic matrix. Currently available composite technology is far behind that of biological composite systems, although it has been recently demonstrated that co-operativity at the inorganic/organic interface can result in complete alignment of inorganic calcite crystals along an identifiable structural feature of organic 10, 12-pentacosadiynoic acid [38]. The present study did not aim at producing control over such a molecular orientation in the composite fabrication.

We selected ionic polymers possessing side-groups such as carboxyl and phosphate as the organic matrix for the HAP crystallization, because these ionizable side-groups have a high affinity for the calcium ions that are a major component of HAP. As expected, the two polymers containing carboxyl and phosphate groups exhibited a significant effect on the coagulation of the HAP suspension as compared with the other ionic polymers, as is demonstrated in Table I. Also in the kinetic study of HAP deposition from aqueous solutions of oversaturated calcium and phosphate ions containing different ionic polymers, PAAc exhibited an interesting effect not shown by the other polymers. PAAc accelerated the nucleation of HAP from highly concentrated calcium and phosphate solutions unless the PAAc concentration in the solutions was very low, as is shown in Table II and Fig. 6 (a and b).

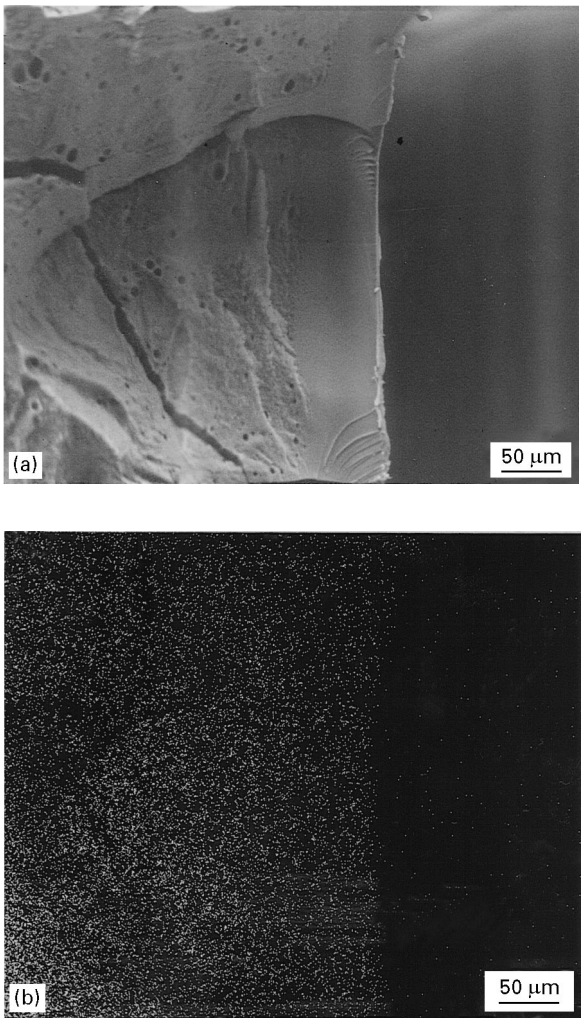

Figure 14 (a) Back-scattered electron image (a) of the fractured surface of a HAP/PAAc-gel composite prepared through *in situ* HAP crystallization and (b) its X-ray image in which the dots denote calcium atoms.

To explain the subtle difference in the kinetic parameters among the polymers used, further studies are needed, but the very low rate of transformation observed when PAA was added may be due to a strong ionic interaction of the cationic polymer chain with the HAP surface. The formation of an amorphous calcium phosphate (ACP) precursor was not detected in the present study. Boskey and Posner [39] have also reported that HAP microcrystallites are directly precipitated from the metastable solution with a low supersaturation. When the solution before mixing had a higher degree of supersaturation (system II), ACP was formed as a precursor, which was subsequently converted to the crystalline HAP through solution-mediated, solid-solid transformation with a release of protons to the outer environment [40, 41]. This process involves dissolution of ACP and the subsequent formation of HAP nuclei with a critical size.

A remarkable difference in solution properties between PAAc and the other ionic polymers used in this study is the extent of polymer solubility in aqueous media containing calcium ions. Amongst the studied polymers only PAAc underwent precipitation from the aqueous solution when calcium ions were added to the solution. This precipitation takes place as a result of irreversible binding of calcium to the PAAc chains.

This point is supported by the IR spectra of patterns (a–e) shown in Fig. 10. The PAAc precipitates formed after the calcium binding may provide a favourable site for HAP crystallization, both nucleation and growth, because the chemisorption of calcium ions into the PAAc gel-like network structure may reduce the free energy for formation of the critical nuclei. A previous study [30] revealed that calcium-binding anionic polymers chemically immobilized onto the surface of a polymer substrate could effectively induce *in situ* formation of HAP microcrystallites in a physiologic environment, thus allowing the formation of a thin HAP layer on the substrate surface with a high adhesion to the substrate. It has also been reported that noncollagenous matrix proteins such as osteonectin [19], bone Gla protein [16], and dentin phosphoprotein [17] accelerate calcium phosphate crystallization when immobilized onto solid support matrices. On the other hand, Termine *et al.* [15] reported that sodium polyacrylate inhibited the amorphous–crystalline transformation of HAP in solution. The retarding effect of PAAc addition on HAP deposition in system I, shown in Fig. 6a, may be due to reasons other than the PAAc precipitation. In this low polymer concentration range, no appreciable precipitation of PAAc was observed. The calcium ions in this case have probably not been taken into solution by the PAAc, which results in a decrease in the calcium concentration in the solution. It is also possible that PAAc chains have been adsorbed onto the surface of immature or growing HAP crystals and have thus retarded the HAP crystallization. The assumption that the precipitated PAAc provides a good surface for HAP deposition is supported by the results presented in Figs 7 (a and b) and 8 (a and b). With an increase in the molecular weight of PAAc the polymer precipitation takes place more readily. Since the incorporation of a small amount of MPOP unit into the PAAc chain renders PAAc water-soluble, even when calcium binding occurs, AAc copolymerization with the MPOP monomer will prevent PAAc precipitation even if calcium ions are present.

As is evident from the IR spectra of patterns (a–e) shown in Fig. 10, the HAP deposits formed in system II in the presence of PAAc contain PAAc. The absence of any indications of PAAc in the IR spectra presented as patterns (a) and (b) in Fig. 9 must be due to a very low PAAc content in the deposits. This is probably due to the point that the PAAc concentration in the starting solution is low (0.02 mM) in comparison with the concentration of calcium (4 mM) and phosphate (2.4 mM). The XRD result for the HAP deposits also supports the incorporation of PAAc into the HAP deposits. As the diffraction patterns (a–f) of Fig. 11 demonstrates, the addition of PAAc and the AAc-MPOP copolymer to the calcium phosphate solutions gave solids that produced more diffuse diffraction patterns, which is probably caused by the incorporation of the polymers into the HAP. There is no information on how the polymer chains are associated with the HAP crystals.

A number of methods are possible for HAP/PAAc composite fabrication. The simplest may be the physical mixing of HAP powders with PAAc in the solid or liquid state. As is apparent from Fig. 3, physical mixing of the two powders yielded a very brittle composite with an inhomogeneous structure. On the other hand, HAP crystallization in solutions containing PAAc gave a HAP deposit with incorporated PAAc chains. The XRD results presented in Fig. 11 imply that there is a strong interaction between HAP and PAAc, since the XRD patterns for HAP precipitates obtained both in the absence and presence of PAAc show significant differences. The adsorption of PAAc chains onto the HAP crystalline surface will disrupt any further HAP crystallization, but will allow the formation of well-mixed composites. As can be observed in Fig. 14, the fractured surface of the composite fabricated through *in situ* crystallization of HAP inside a three-dimensional PAAc gel placed in an aqueous medium containing oversaturated calcium and phosphate ions shows a fine dispersion of HAP in the composite. The tensile testing results shown in Fig. 13 also reveal that the *in situ* fabricated composite is different from the physically mixed composite. As mentioned above, strong adhesion of *in situ* formed HAP crystals onto the MPOP polymer chains grafted to a solid polymer surface was reported in a previous paper [30]. A more detailed study on the *in situ* formation of composites is at present under way.

5. Conclusions

The spontaneous precipitation and amorphous-crystalline tansformation of HAP were affected by the presence of anionic and cationic synthetic polymers through molecular interactions of the polymer chains with inorganic components. These kinetic parameters varied depending on the chemistry, concentration, and molecular weight of the polymers added and the supersaturation of the system with regard to HAP. In contrast to the other polymers used, PAAc accelerated the nucleation of HAP from highly concentrated calcium and phosphate solutions. This acceleration was due to PAAc precipitation as a result of irreversible calcium binding to the polymer chains, which may provide a favourable site for the nucleation and growth of HAP crystallites. The high affinity for calcium ions was confirmed by the fact that the polymers carrying carboxylic acid and phosphate have a significant effect on the coagulation of HAP suspension. As a consequence of *in situ* crystallization of HAP in the presence of PAAc, the polymer chains were incorporated to the microcrystalline aggregates. The HAP/PAAc composite prepared through *in situ* HAP crystallization in the presence of PAAc was superior to that obtained by simple physical mixing with regard to the wet state mechanical properties and homogeneity in mixing.

Acknowledgements

The authors thank Mr. K. Okunaga and Mr. H. Shibuya, Nippon Electric Glass Co Ltd., Shiga, Japan, for their contribution to the powder X-ray diffraction analysis.

References

1. S. MANN, D. D. ARCHIBALD, J. M. DIDYMUS, T. DOUGLAS, B. R. HEYWOOD, F. C. MELDRUM and N. J. REEVES, *Science* **261** (1993) 1286.
2. S. MANN, *Nature* **365** (1993) 499.
3. B. C. BUNKER, P. C. RIEKE, B. J. TARASEVICH, A. A. CAMPBELL, G. E. FRYXELL, G. L. GRAFF, L. SONG, J. LIU, J. W. VIRDEN and G. L. McVAY, *Science* **264** (1994) 48.
4. J. J. M. DAMEN and J. M. TEN CATE, *J. Dent. Res.* **71** (1992) 453.
5. *Idem*, *ibid.* **68** (1989) 1355.
6. J. D. TERMINE and K. M. CONN, *Calcif. Tiss. Res.* **22** (1976) 149.
7. J. D. SALLIS, M. R. BROWN and N. M. PARKER, in "Surface reactive peptides and polymers" ACS Symposium Series No. 444, edited by M. J. Comstock, (American Chemical Society, Washington, DC, 1991) p. 149.
8. D. SKRTIC and E. D. EANES, *Calcif. Tiss. Int.* **50** (1992) 55.
9. A. L. BOSKEY and B. L. DICK, *ibid.* **49** (1991) 193.
10. B. R. HEYWOOD and E. D. EANES, *ibid.* **50** (1992) 149.
11. S. KOUTSOPOULOS, J. DEMAKOPOULOS, X. ARGIRIOU, E. DALAS, N. KLOURAS and N. SPANOS, *Langmuir* **11** (1995) 1831.
12. W. J. LANDIS, M. J. SONG, A. LEITH, L. McEWEN and B. F. McEWEN, *J. Struct. Biol.* **110** (1993) 39.
13. B. R. HEYWOOD, N. H. C. SPARKS, R. P. SHELLIS, S. WEINER and S. MANN, *Connective Tissue Res.* **25** (1990) 103.
14. J. P. GORSKI, *Calcif. Tiss. Int.* **50** (1992) 391.
15. J. D. TERMINE, R. A. PECKAUSKAS and A. S. POSNER, *Arch. Biochem. Biophys.* **140** (1970) 318.
16. A. LANDIS, A. LUSSI and M. A. CRENSHAW, *Calcif. Tiss. Int.* **44** (1989) 286.
17. Y. DOI, T. HORIGUCHI, S.-H. KIM, Y. MORIWAKI, N. WAKAMATSU, M. ADACHI, H. SHIGETA, S. SASAKI and H. SHIMOKAWA, *ibid.* **52** (1993) 139.
18. D. J. WHITE and E. R. COX, in "Surface reactive peptides and polymers", ACS Symposium Series No. 444, edited by M. J. Comstock (American Chemical Society, Washington, DC, 1991) p. 177
19. J. D. TERMINE, H. K. KLEINMAN, S. W. WHITSON, K. M. CONN, M. L. McGARVEY and G. R. MARTIN, *Cell* **26** (1981) 99.
20. A. VEIS, B. SABSAY and C. B. WU, in "Surface reactive peptides and polymers", ACS Symposium Series No. 444, edited by M. J. Comstock (American Chemical Society, Washington, DC, 1991) p. 1.
21. C. S. SIKES, M. L. YEUNG and A. P. WHEELER, *ibid.* p. 50.
22. E. MUELLER and C. S. SIKES, *Calcif. Tiss. Int.* **52** (1993) 34.
23. T. AOBA and E. C. MORENO, in "Surface reactive peptides and polymers", ACS Symposium Series No. 444, edited by M. J. Comstock (American Chemical Society, Washington, DC, 1991) p. 85.
24. L. ADDADI, J. MORADIAN-OLDAK and S. WEINER, *ibid.* p. 13.
25. M. TANAHASHI, T. YAO, T. KOKUBO, M. MINODA, T. MIYAMOTO, T. NAKAMURA and T. YAMAMURO, *J. Biomed. Mater. Res.* **29** (1995) 349.
26. S. I. STUPP and G. W. CIEGLER, *ibid.* **26** (1992) 169.
27. A. M. RADDER, H. LEENDERS and C. A. van BLITTERSWIJK, *ibid.* **28** (1994) 141.
28. K. R. ROGERS and S. W. SHALABY, in "Polymers of biological and biomedical significance," ACS Symposium Series No. 540, edited by S. W. Shalaby, Y. Ikada, R. Langer and J. Williams, (American Chemical Society, Washington, DC, 1994) p. 116.
29. E. DALAS, J. K. KALLITSIS and P. G. KOUTSOUKOS, *Langmuir* **7** (1991) 1822.
30. O. N. TRETINNIKOV, K. KATO and Y. IKADA, *J. Biomed. Mater. Res.* **28** (1994) 1365.
31. E. DALAS, J. KALLITSIS and P. G. KOUTSOUKOS, *Colloids Surf.* **53** (1991) 197.
32. K. KATO, Y. EIKA and Y. IKADA, *J. Biomed. Mater. Res.* **32** (1996) 687.
33. P. CALVERT, in "Biomolecular materials by design," Materials Research Symposium Proceedings Vol. 330, edited by M. Alper, H. Bayley, D. Kaplan and M. Navia (Materials Research Society, Pittsburgh, PA, 1994) p. 79.
34. W. BONFIELD, in "Bioceramics: materials characteristics versus *in vivo* behaviour", Annals of the New York Academy of Sciences Vol. 523, edited by P. Ducheyne and J. E. Lemons (New York, 1988) p. 173.
35. O. LINDBERG and L. ERNSTER, *Methods Biochem. Anal.* **3** (1956) 1.
36. J. D. TERMINE and A. S. POSNER, *Nature* **211** (1966) 268.
37. M. OKAZAKI, Y. MORIWAKI, T. AOBA, Y. DOI and J. TAKAHASHI, *Caries Res.* **15** (1972) 477.
38. A. BERMAN, D. J. AHN, A. LIO, M. SALMERON, A. REICHERT and D. CHARYCH, *Science* **269** (1995) 515.
39. A. L. BOSKEY and A. S. POSNER, *J. Phys. Chem.* **80** (1976) 40.
40. *Idem*, *ibid.* **77** (1973) 2313.
41. P. KOUTSOUKOS, Z. AMJAD, M. B. TOMSON and G. H. NANCOLLAS, *J. Amer. Chem. Soc.* **102** (1980) 1553.

Received 13 November 1995
and accepted 18 February 1997